Application of learning vector quantization for estimating size and position of metallic particle adhering to spacer in GIS

YASIN KHAN
Department of Electrical Engineering, College of Engineering, King Saud University, P.O. Box. 800, Riyadh 11421, Kingdom of Saudi Arabia.

Metallic particle is the most harmful material in the perspective of Gas-Insulated Substation (GIS) reliability. It creates defects in GIS, especially in the weakest areas, i.e. the triple junction, by initializing partial discharges (PDs) which can lead to the failure of GIS. Therefore, the investigation of PD characteristics and particle size and position on the spacer surface are indispensable in the efforts of improving the reliability of GIS equipments. In this paper, learning vector quantization (LVQ) was employed to recognize various PD signal patterns provoked by different particle sizes and positions on the spacer surface and processed the PD patterns to estimate the particle size and position in simulated GIS arrangement. With its pattern recognition capability, the developed LVQ technique was able to perform such estimations with an accuracy of 76%. The proposed method is designated as a contribution towards reliability improvement of GIS systems.

(Received April 6, 2015; accepted May 7, 2015)

Keywords: Learning vector quantization (LVQ), GIS, Partial discharge, Particle size and position estimation

1. Introduction

SF_6 has received worldwide acceptance for use in various high-voltage tools because of its superior insulating properties, such as compactness, extraordinary dielectric strength, outstanding arc quenching properties, non-flammability, non-toxicity along with advanced heat transfer characteristics [1-3]. However, the reliability of GIS is subject to the deterioration caused by the existence of metal particles. Due to charging of the insulators, free metal particles can stick to spacer of the GIS creating serious defects. As a consequence of these defects, PDs can commence in SF_6 [4-5]. Such PDs are very dangerous to the insulation integrity of the GIS. The severity and the PD pattern depend on the particle's length and position on the spacer surface [6-8]. Hence, it is important to recognize the size and location of particle along the spacer [9]. A subsequent study by the authors with more advance algorithm, i.e. Artificial Neural Network (ANN), has also been conducted with better accuracy [10].

In present study, Learning Vector Quantization (LVQ) algorithm is proposed for particle size and position estimation purpose. LVQ is supervised classification algorithm invented by T. Kohonen [11]. Until now, the application of LVQ is limited to general PD classification for recognizing various defects [12-13]. None of them focused on particle defect in GIS.

The development of LVQ was preceded by PD quantities generated at several particle dimensions and locations. For PD shapes characterization, a number of statistical operators called "fingerprint" were established. LVQ was implemented by using built-in toolbox of MATLAB version R2010a. The results show that the best-developed LVQ network in this study is capable of achieving 76% recognition accuracy.

2. Experimental setup

The system studied is a parallel-plane electrode surrounded in a chamber having SF_6 gas. An experimental setup is shown in **Figure 1**. The particle size is represented as *L* whereas the particle location *H* is well-defined as the distance among the bottom tip of the particle and the lower (i.e. grounded) electrode. The experimental setup shown in **Figure 2** and procedure is explained in detail in [9].

The PD detection device bandwidth was fixed from 20 kHz to 300 kHz for PD measurements. After calibrating the system, it computes and shows the floor noise and permits the amplifier limits to be adjusted without disturbing the system calibration.

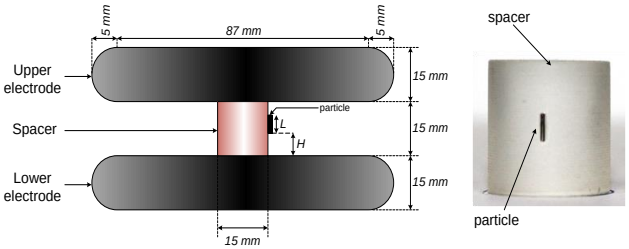

(a) The arrangement (b) The appearance

Fig. 1. The tested electrode-spacer system

There are 10 arrangements of the particle lengths (*L*) and positions (*H*) have been used in research. For ease of analysis, they are named as "Defect 1" to "Defect 10", as shown in **Figure 3**. In order to include the effect of SF_6

pressure, PD data was collected for each defect at SF_6 pressures of 1, 1.5, 2, 2.5, and 3 bars. For each of these cases, the measurement was carried out 4 times to provide enough data for training process of the developed BP-ANN. Therefore, a total of 200 PD measurements were obtained. Each PD pattern acquisition process in every measurement was set about 10 seconds. For comparison among PD patterns of different defects, PDs data collection were carried out by the constant voltage i.e. 35 kV_{rms}.

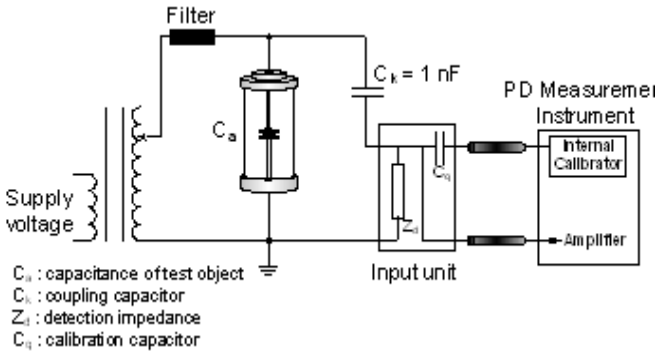

Fig. 2. The schematic diagram of the experimental setup based on the IEC 60270 PD detection method.

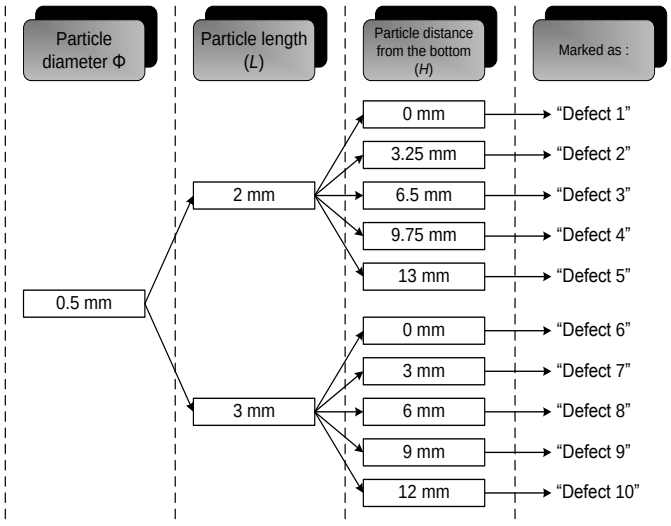

Fig. 3. The various combinations of particle size and position that form the defects 1 to 10

3. PD Signals Acquisition and Presentation

A set of experimental data having the evidence of every PD pulse were processed using data-processing application developed with MATLAB software. The following PD distributions were calculated for every experimental result.

(a) Maximum PD magnitude against phase angle ($H_{qmax}(\phi)$)
(b) Average PD magnitude against phase angle ($H_{qn}(\phi)$)
(c) PD counts against phase angle ($H_n(\phi)$)
(d) PD counts against magnitude ($H(q)$)
(e) PD counts against energy ($H(p)$)

A typical graphical representation of these PD distributions is shown in Fig. 4. Out of five PD distributions, the first three can be separated into two different distributions for negative and positive cycles of the applied alternating voltage. Hence, for positive cycle the obtained distributions become $H_{qmax}^{+}(\phi)$, $H_{qn}^{+}(\phi)$, and $H_n^{+}(\phi)$, and for negative half-cycle the distributions become $H_{qmax}^{-}(\phi)$, $H_{qn}^{-}(\phi)$, and $H_n^{-}(\phi)$.

As indicated in section I, the PD signals are identified by their "fingerprints", which are the groups of numerous statistical operators quantitatively describing the PD distributions presented in Figure 4. The statistical operators used in this work, contain "skewness", "kurtosis', "peaks", "asymmetry", "cross correlation" and "phase factor" [10]. The results shown in Figure 4, the applicable operators are listed in Table 1. As shown in this table, there are 29 operators recorded from every PD signal. The typical values of these operators are shown in Fig. 5. The 29 operators listed in Table 1 are called "Operator 1" to "Operator 29" in this study according to Figure 5, with "skewness" of $H_{qmax}(\phi)$ and "kurtosis" of $H(p)$ being "Operator 1" and "Operator 29", respectively. Since the PD measurements for every defect has been performed 4 times at 5 SF_6 pressure values, each defect was represented by a fingerprint data matrix of 29 × 20 size.

4. Applications of LVQ for particle size and position estimation

LVQ is one of the neural network algorithms which is capable of performing multiclass classification. It is basically similar to Self-Organizing Map, developed also by Kohonen, however the training process of competitive layers is done in a supervised manner, i.e. target outputs are defined [11]. Thus, during the learning process input pattern vectors are classified into target classes chosen by the user.

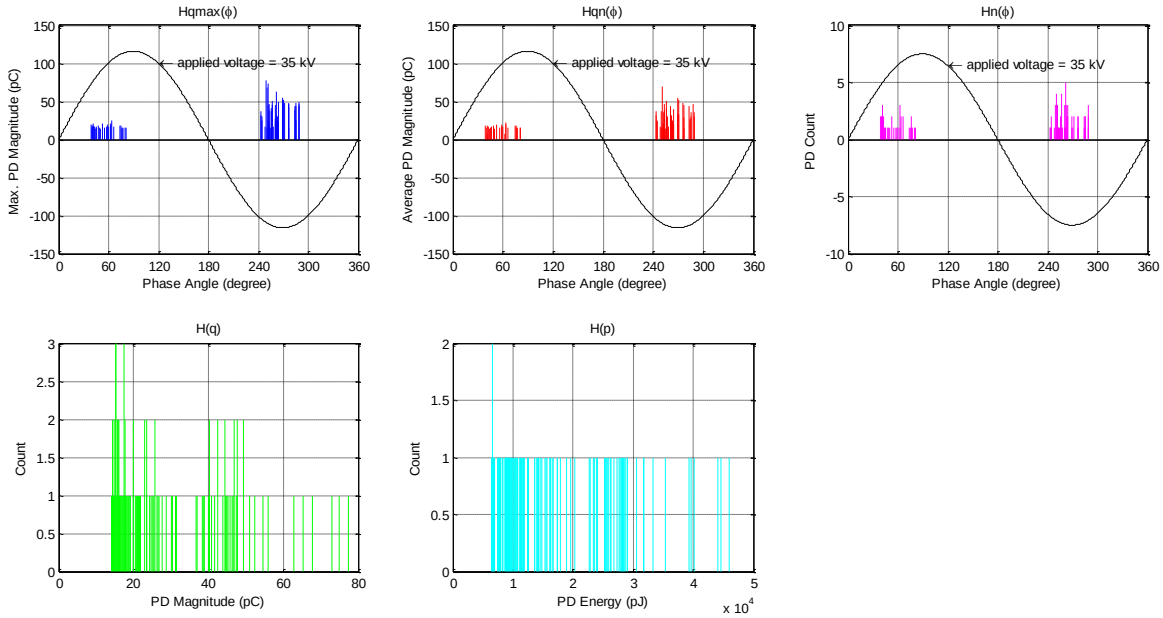

Fig. 4 PD Distributions of Defect 2 obtained from the first measurement at SF_6 pressure of 3 bars

Table 1. Applicable statistical operators for each PD distribution

PD Distrib.	Skewness	Kurtosis	Peaks	Asymmetry	Cross Cor.	Phase Fact.	#
$H_{qmax}(\phi)$	(+) & (-)	(+) & (-)	(+) & (-)	✓	✓	×	8
$H_{qn}(\phi)$	(+) & (-)	(+) & (-)	(+) & (-)	✓	✓	✓	9
$H_{n}(\phi)$	(+) & (-)	(+) & (-)	(+) & (-)	✓	✓	×	8
$H(n)$	✓	✓	×	×	×	×	2
$H(p)$	✓	✓	×	×	×	×	2
Total number of statistical operators							**29**

Note: ✓*denotes "Yes", whereas* × *represents "No".*

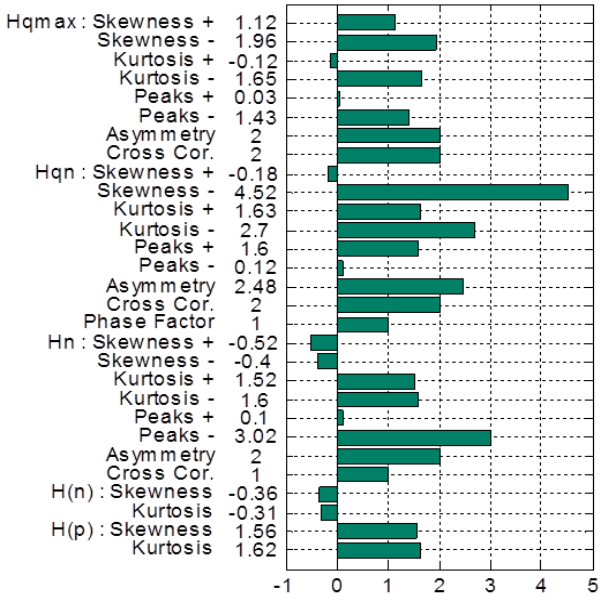

Fig. 5. The statistical operators making up the PD fingerprints

A LVQ network consists of two layers, namely competitive layer and linear layer, as shown by the structure in Fig. 6. During the training (learning), the network learns distribution and topology of the input vectors. The elements in the vector inputs are arranged according to the topology determined by the user, which can be random topology. The distances among elements are obtained with distance function. Link distance is the most common distance function usually used.

LVQ identifies and declares the nearest neuron i^* as a winner. However, during the training all neurons in neighby area $N_{i^*}(d)$ are updated using Kohonen rule, except the winning neuron. All these neurons $i \in N_{i^*}(d)$ are adjusted using the following procedures:

$$ {}_i IW\{1,1\}(q) = {}_i IW\{1,1\}(q-1) + \alpha(p(q) - {}_i IW\{1,1\}(q-1)) \quad (1)$$

Or

$$ {}_i IW\{1,1\}(q) = (1-\alpha)\,{}_i IW\{1,1\}(q-1) + \alpha p(q) \quad (2)$$

Thus, the $N_{i^*}(d)$ has the indices for all neurons which are located in a radius d of the winning neuron i^*.

$$N_i(d) = \{j, d_{ij} \le d\} \quad (3)$$

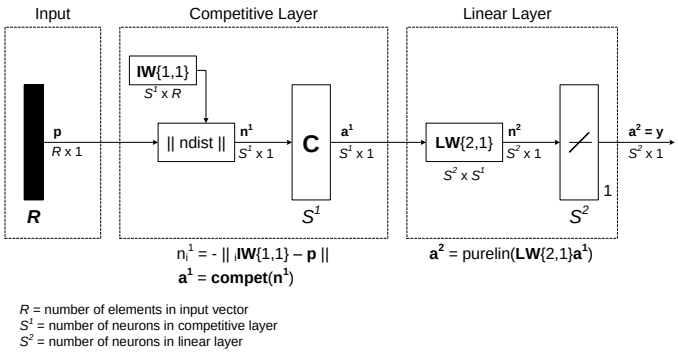

Fig. 6 The LVQ network architecture

Therefore, when vector *p* is presented, the weights of winning neuron and its neighbors move toward *p*. As a result, after certain number of iterations, neighboring neurons have vectors alike each other.

In this study, the learning process described above, also called LVQ1 learning rule, is further improved by using LVQ2.1 learning rule. The built-in LVQ toolbox in MATLAB version R2010a was used to implement the described LVQ network. In developing the best network, the learning rate α and the number of neurons in competitive layers S^1 are varied in the wide ranges. The value of α is varied between 0.0025 and 0.11 with a step of 0.0025 and the value of S^1 is varied between 5 and 50. With such a "grid search" method, the chance to obtain the best LVQ network becomes higher.

Since there are 10 defects to be recognized, the developed LVQ network output will consist of 10 classes. Out of 4 PD fingerprint dataset obtained from 4 measurements for each defect, 3 of them are used for training (learning) and the remaining 1 is used for testing. Therefore, there are 50 recognitions performed by the developed LVQ network because there are 5 pressure values. If the network can recognize a certain testing data set same as it is trained for, then "succeed" is achieved. Otherwise, "fail" is obtained. The performance of the developed LVQ network is expressed in terms of accuracy, which is the number of "succeed" occurrences divided by 50.

Fig. 7 show the performance of the developed LVQ network using several values of α and S^1. The highest accuracy achieved by the network is 76%. This accuracy could be achieved by using several values of learning rate α, however with different number of competitive neurons. Therefore, the chosen network is the one which can achieve 76% accuracy with the lowest number of competitive neurons, i.e. the network whose performance is shown in Fig. 7. This is because lower number of competitive neurons can reduce the network complexity, which results in lower computation time. As indicated in Fig. 7, the network achieves 76% accuracy when it is built using a learning rate of 0.0275 and 33 competitive neurons. The detailed results of this network, which is the list of "succeed"/"fail" occurrences, is presented in Table 2.

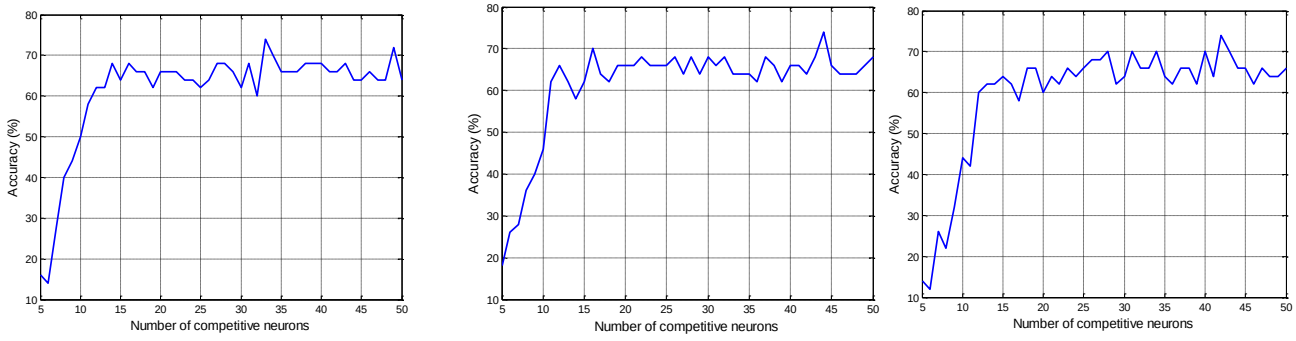

(a) α = 0.0275 (b) α = 0.035 (c) α = 0.045

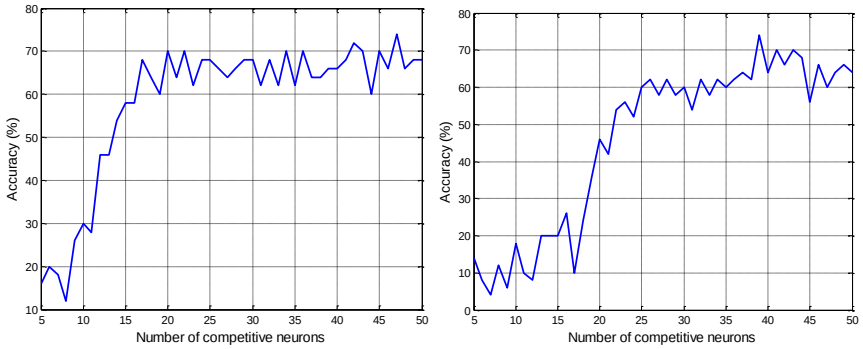

(d) α = 0.055 (e) α = 0.095

Fig. 7 Accuracies achieved by the developed LVQ network with various learning rates

5. Conclusions

The PD signals produced by particle of various sizes and changing its position to the spacer surface were attained by the Digital PD Detector. Utilizing the acquired PD pulses data, various PD distributions, including time-resolved and phase-resolved PD distributions were calculated. The PD patterns were characterized by their fingerprint values, consisting of some statistical operators. The Learning Vector Quantization (LVQ) algorithm with LVQ2.1 learning rule was developed and implemented in MATLAB software for recognition of the obtained PD patterns. In order to obtain the most optimal BP-ANN, several parameters were varied, including the value of learning ratio and the density of neurons in competitive layer. The network with learning rate of 0.0275 was found to be the most optimal since it can achieve the highest accuracy, i.e. 76%, with the lowest number of competitive neurons.

Table 2. The recognition result produced by the developed LVQ with a = 0.0275 and S1 = 33

Tested defect	The recognition results				
	1 bar	1.5 bars	2 bars	2.5 bars	3 bars
Defect 1	✓	×	✓	×	×
Defect 2	✓	✓	×	×	✓
Defect 3	✓	✓	×	✓	✓
Defect 4	×	×	✓	✓	✓
Defect 5	✓	✓	✓	✓	✓
Defect 6	✓	✓	×	✓	✓
Defect 7	✓	✓	✓	✓	✓
Defect 8	×	✓	×	✓	✓
Defect 9	✓	×	✓	✓	✓
Defect 10	✓	✓	✓	✓	✓

Note: ✓ denotes "succeed", whereas × represents "fail".

Acknowledgements

The authors would like to extend their sincere appreciation to the Deanship of Scientific Research (DSR) at King Saud University for its funding of this research through the Research Group Project No. RG-1436-012.

References

[1] H. Anis, High Voltage Engineering : Theory and Practice, M. Khalifa, Ed. New York, NY: Marcel Dekker, Inc., 1990, pp. 243-273.

[2] P. Bolin, Electric Power Substations Engineering, J.D. McDonald, Ed. Boca Raton, FL: Taylor & Francis Group, LLC, 2007.

[3] H. S. Jain, Handbook of Switchgears, B.H.E. Limited, Ed. New York, NY: McGraw-Hill, 2007.

[4] M. M. Morcos, S. A. Ward, H. Anis, K. D. Srivastava, and S. M. Gubanski. IEEE Electrical Insulation Magazine, **16**(5), 25 (2000).

[5] H. Okubo, K. Nishizawa, T. Okusu, N. Hayakawa, F. Endo, M. Yoshida, K. Uchida. Annual Report Conference on Electrical Insulation and Dielectric Phenomena (CEIDP), pp. 395-399, 26-29 Oct. 2008.

[6] N. Kanako, T. Okusu, H. Kojima, N. Hayakawa, F. Endo, M. Yoshida, K. Uchida, H. Okubo. International Conference on Condition Monitoring and Diagnosis (CMD), pp. 443-447, April 2008.

[7] N. Hayakawa, T. Okusu, K. Nishizawa, H. Kojima, F. Endo, M. Yoshida, K. Uchida, H. Okubo. International Conference on Condition Monitoring and Diagnosis (CMD), pp. 46-50, 21-24pril 2008.

[8] Y. Negara, K. Yaji, K. Imasaka, N. Hayashi, J. Suehiro, M. Hara. IEEE Transactions on Dielectrics and Electrical Insulation, **14**(1), 91 (2007).

[9] Y. Khan, F. N. Budiman, A. Beroual, N. H. Malik, A. A. Al-Arainy, The European Physical Journal Applied Physics., **62,**. 20801p1 (2013).

[10] F. N. Budiman, Y. Khan, A. Beroual, N. H. Malik, A. A. Al-Arainy, IEEE Transactions on Dielectrics and Electrical Insulation. **20**(6), 2143 (2013)

[11] T. Kohonen, Proceedings of the IEEE, **78**(9), 1464 (1990).

[12] E. Gulski, A. Krivda, IEEE Transactions on Electrical Insulation, **28**(6), 984 (1993).

[13] A. A. Mazroua, R. Bartnikas, M. M. A. Salama, IEEE Transactions on Electrical Insulation **1**(6), 1119 (1994).

*Corresponding author: yasink@ksu.edu.sa